

## Article

# Remote Sensing and Field Data Analysis to Evaluate the Impact of Stone Bunds on Rainfed Agriculture in West Africa

Meron Lakew Tefera <sup>1,2</sup>, Hassan Awada <sup>1,3,\*</sup>, Mario Pirastru <sup>1,2,3</sup> , James Mantent Kombiok <sup>4</sup> , Joseph Adjebeng-Danquah <sup>5</sup> , Ramson Adombilla <sup>5</sup>, Peter Anabire Asungre <sup>5</sup> , George Mahama <sup>5</sup>, Alberto Carletti <sup>6</sup>  and Giovanna Seddaiu <sup>1,2</sup> 

<sup>1</sup> Department of Agricultural Sciences, University of Sassari, Viale Italia 39, 07100 Sassari, Italy; mltefera@uniss.it (M.L.T.); mpirastru@uniss.it (M.P.); gseddaiu@uniss.it (G.S.)

<sup>2</sup> Desertification Research Centre, NRD, University of Sassari, Viale Italia 57, 07100 Sassari, Italy

<sup>3</sup> National Biodiversity Future Centre (NBFC), 90133 Palermo, Italy

<sup>4</sup> Kundok Development Consult (KDC), No 1 Target Avenue, Vittin Residential Area, Tamale P.O. Box TL 7022, Ghana; kombiokjm@yahoo.com

<sup>5</sup> CSIR-Savanna Agricultural Research Institute, Nyankpala (SARI), Tamale P.O. Box 52, Ghana; ja.danquah@csir.org.gh (J.A.-D.); ramson50yahoo@gmail.com (R.A.); anabire@gmail.com (P.A.A.); yakubu.mg@gmail.com (G.M.)

<sup>6</sup> Department of Civil, Environmental Engineering and Architecture, University of Cagliari, Via Marengo 2, 09123 Cagliari, Italy; alberto.carletti@unica.it

\* Correspondence: hawada@uniss.it

**Abstract:** This study evaluates the effectiveness of stone bunds in enhancing soil moisture, vegetation health, and crop yields in Ghana's semi-arid Upper East Region, an important area for agricultural productivity in West Africa. In this region, agricultural practices are heavily impacted by erratic rainfall and poor soil moisture retention, threatening food security. Despite the known benefits of traditional soil conservation practices like stone bunds, their effectiveness in this context has not been fully quantified. Field and remote sensing data were used to evaluate the influence of stone bunds on soil moisture dynamics, vegetation growth, and crop yield. Experimental plots with and without stone bunds were monitored for climate, soil water infiltration, and soil moisture and analyzed using the NDVI from Sentinel-2 satellite imagery over two growing seasons under sorghum production (2022–2023). The results indicated that stone bunds enhanced soil moisture retention and increased infiltration rates. The NDVI analysis consistently revealed higher vegetation health and growth in the plots with stone bunds, particularly during critical growth periods. The intermediate results of the conducted experiment indicated that stone bunds increased sorghum yields by over 35% compared to the control plots. The substantial agronomic benefits of stone bunds as a soil and water conservation strategy were evident, improving soil water infiltration, water retention, vegetation health, and crop yields. The findings support the broader adoption of stone bunds in semi-arid regions to enhance agricultural productivity and resilience against climate variability. Further research is recommended to explore the long-term impacts and the integration of stone bunds with other sustainable farming practices to optimize rainfed agricultural outcomes.

**Keywords:** stone bunds; remote sensing; water harvesting; soil moisture; semi-arid regions; NDVI dynamics; soil and water conservation; crop yield improvement



**Citation:** Tefera, M.L.; Awada, H.; Pirastru, M.; Kombiok, J.M.; Adjebeng-Danquah, J.; Adombilla, R.; Asungre, P.A.; Mahama, G.; Carletti, A.; Seddaiu, G. Remote Sensing and Field Data Analysis to Evaluate the Impact of Stone Bunds on Rainfed Agriculture in West Africa. *Land* **2024**, *13*, 1654. <https://doi.org/10.3390/land13101654>

Academic Editor: Le Yu

Received: 7 August 2024

Revised: 30 September 2024

Accepted: 7 October 2024

Published: 10 October 2024



**Copyright:** © 2024 by the authors. Licensee MDPI, Basel, Switzerland. This article is an open access article distributed under the terms and conditions of the Creative Commons Attribution (CC BY) license (<https://creativecommons.org/licenses/by/4.0/>).

## 1. Introduction

Ghana's agriculture sector relies heavily on rainfall, with approximately 70% of the land depending on it for crop water requirements [1]. This sector employs approximately 52% of the workforce, contributes 54% to the gross domestic production, and provides over 90% of the country's food needs, thereby exerting significant pressure on natural resources [2]. In this challenging context, the agricultural sector faces soil degradation,

desertification, and drought, making soil and water conservation (SWC) measures essential for sustainable production [3–7]. In particular, crop farmers in Ghana’s northern region encounter significant challenges due to the unpredictability and intensity of rainfall [8].

Water scarcity is a critical issue in arid and semi-arid regions, where maintaining optimal soil moisture levels is essential for agricultural productivity [9]. Over centuries, agricultural practices and water erosion have significantly degraded soil fertility and altered the hydraulic properties of soil [10–12]. These challenges are exacerbated by a warming climate, posing significant obstacles to sustainable crop production [13]. Recent studies, such as [14,15], underscore the vital role of surface soil moisture in regulating ecological and hydrological processes. Effective soil moisture management is crucial for enhancing crop and livestock productivity in water-limited environments. The hydraulic properties of soil are fundamental in determining both soil and environmental quality and the soil’s capacity to support ecosystem functions [13]. Moreover, soil and water conservation measures, such as stone bunds, pits, half-moons, and contour stones, have proven effective in mitigating water stress and erosion [9,16]. Integrating these conservation practices with sound agronomic techniques can significantly improve agricultural yields and water productivity.

Monitoring soil moisture is crucial for assessing the impact of water harvesting techniques in rainfed agriculture, providing valuable insights into soil water capacity and moisture distribution. However, field-based monitoring presents significant financial and logistical challenges due to the vast agricultural landscapes, leading to common data scarcity. To address this issue, integrating remote sensing data, particularly the Normalized Difference Vegetation Index (NDVI), offers a promising solution [17–19]. The NDVI provides a comprehensive perspective on vegetation health and vigor, serving as a proxy for soil moisture effects on vegetation in rainfed agricultural systems [20,21]. Studies integrating the NDVI with on-field soil moisture measurements have successfully identified crop water stress periods and enhanced agricultural water management understanding [22–24]. Combining the NDVI data with ground-based observations allows for researchers to extend their findings to larger areas, offering a holistic view of water harvesting techniques like stone bunds across varied landscapes. This interdisciplinary approach holds immense potential for informing water management strategies, optimizing crop yields, and promoting sustainable agricultural practices in regions characterized by rainfall variability and limited data access [25].

Stone bunds are widely recognized for their effectiveness in mitigating surface runoff and managing soil erosion. They are the predominant techniques adopted by farmers across West Africa due to their ability to promote sedimentation and soil infiltration and to increase moisture retention [26,27]. The effectiveness of stone bunds depends on several factors, including climatic conditions, design, soil characteristics, and crop selection [14,16]. The adoption of these structures has significantly improved crop yields, annual income, and the livelihoods of smallholder farmers [28]. Research by [29–32] demonstrates substantial yield increases in areas utilizing stone bunds, with some studies reporting yield increases ranging from two to three times compared to control areas [31].

Previous research in West Africa has predominantly focused on yield, soil fertility, and erosion [16,33–35]. However, there is a notable gap in addressing the impact of stone bunds on enhancing soil moisture. Additionally, most of these studies are limited to small-scale, localized field analyses, with a scarcity of research specifically examining the effectiveness of stone bunds in Ghana. This study aims to address these gaps and provide, through integrated field data and remote sensing analysis, valuable insights into the effects of stone bunds on soil moisture retention and agricultural productivity in Ghana.

The specific objectives are the following:

1. Examine the influence of stone bunds on soil moisture dynamics.
2. Evaluate the effect of stone bunds on vegetation growth using NDVI data on a large spatial scale.

- Analyze the relationship between stone bunds, environmental factors, and agricultural productivity.

## 2. Materials and Methods

### 2.1. Study Area

The experiment was conducted in Nangodi (Soliga) Nabdam district, located in the Upper East Region of Ghana, at coordinates  $10^{\circ}51'10.44''$  N,  $0^{\circ}40'12.72''$  W, with an elevation of 198.6 m (Figure 1). This area is part of Ghana's savanna zone and experiences a semi-arid climate characterized by distinct wet and dry seasons. Rainfall in this region is typically lower compared to the southern part of Ghana, with the rainy season extending from May to October, averaging 1039 mm annually between 1981 and 2023 according to NASA (2024). Stone bunds, widely used for soil and water conservation, are prevalent in the region. A survey with local experts and farmers revealed that the stone bunds in the experimental plots ranged from 20 to 30 years old and have been consistently maintained according to local farmers' practices.

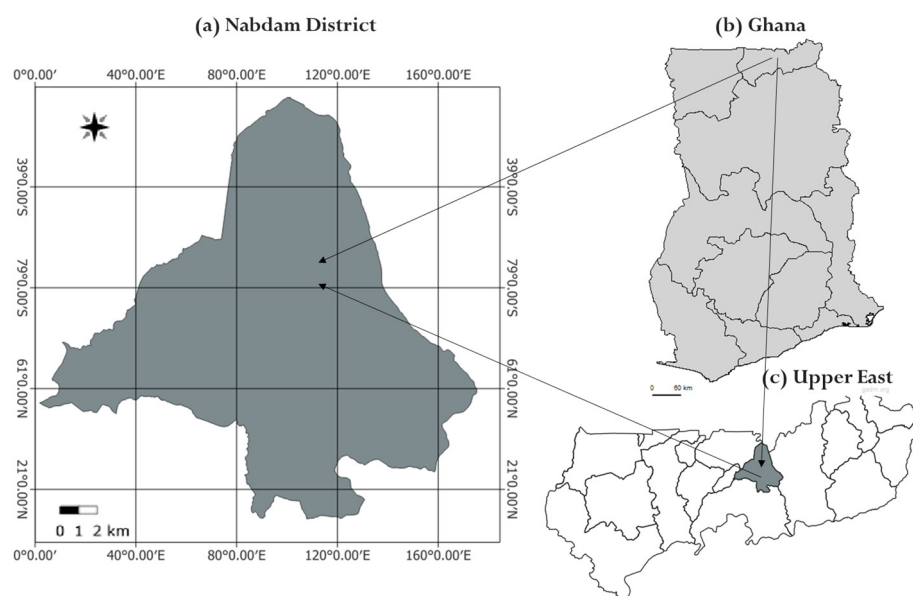


**Figure 1.** Location of the experimental site in the Upper East Region, Nabdam District (a), specifically in Nangodi (Soliga) (c), Ghana (b).

### 2.2. Soil Data

In the top 10 cm layer, the soil texture is predominantly loam, with high levels of organic matter and active biological processes. As the depth increases, the soil transitions to clay loam at 10–20 cm and 20–30 cm and to clay at 30–40 cm. This gradation is accompanied by a decrease in organic matter, total nitrogen, and phosphorus levels, while the C/N ratio increases (Table 1). The topsoil's bulk density was observed as  $1.37 \text{ g/cm}^3$ , which corresponds to the typical range for loam soils [36]. Based on the observed soil properties, the soils in the study area are classified as Alfisols, specifically Ustalfs, according to [37]. These soils are characteristic of semi-arid regions, with high base saturation and fertility. The loam texture in the top layers and the transition to clay loam and clay at deeper depths further support this classification.

**Table 1.** Soil texture and chemical characteristics across different depths (April 2022).

Soil Depth	Soil Texture	pH (H <sub>2</sub> O)	Organic Matter (g·Kg <sup>-1</sup> )	Total N (g·Kg <sup>-1</sup> )	C/N (g·Kg <sup>-1</sup> )	P <sub>2</sub> O <sub>5</sub> (mg·Kg <sup>-1</sup> )	K <sub>2</sub> O (mg·Kg <sup>-1</sup> )
0–10	Loam	6.3	26	1.3	12	9	150
20–30	Clay Loam	6.3	21	0.9	13	5	89
20–30	Clay Loam	6.2	9	0.6	8	5	14
30–40	Clay	6.2	9	0.4	13	4	28

### 2.3. Experimental Plots

Two experimental plots were established for evaluating the soil moisture dynamic and crop productivity: a treatment plot with stone bunds and a control plot without stone bunds serving as a comparative baseline. Each plot was equipped with two WaterScout SMEC 300 Soil Moisture sensors, installed centrally to monitor moisture levels at 10 cm and 20 cm depths. Soil moisture data were recorded at 15 min intervals throughout the study period. Additionally, a WatchDog 2800 Series Weather Station was installed on-site to record weather parameters at the same intervals. Figure 2 provides a graphical overview of the stone bunds, including their dimensions and the placement of moisture sensors (MSP) within the study area.

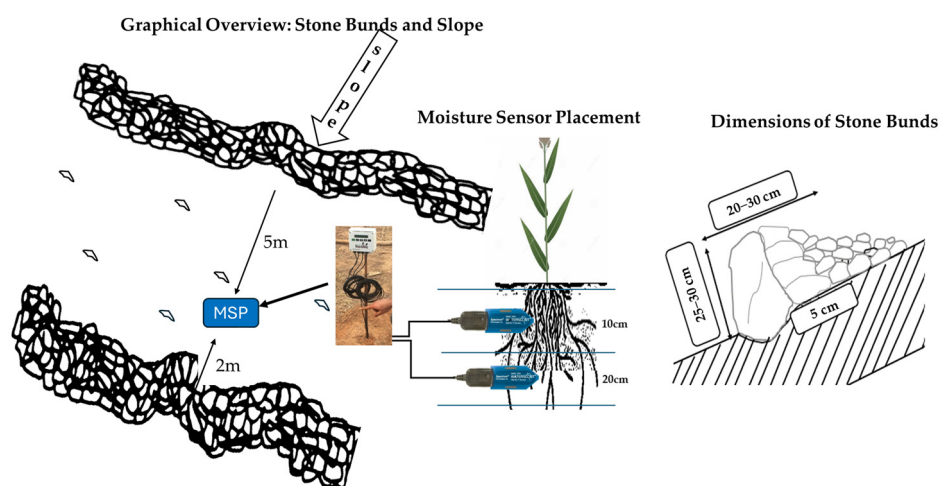


**Figure 2.** Graphical overview of stone bunds installed in the study area: dimensions and moisture sensor placement (MSP).

Weather data, including rainfall (R), temperature (T), relative humidity, wind speed, wind gusts, and solar radiation, were collected for both the 2022 and 2023 growing seasons to understand the environmental conditions affecting crop growth. Cumulative rainfall during the study period was recorded at 1002 mm in 2022 and 871 mm in 2023. Average temperatures were monitored and showed an increase from 27.2 °C in 2022 to 27.8 °C in 2023. Relative humidity levels were also tracked, rising slightly from 80% to 82% over the two years. Wind conditions were measured, revealing a decrease in wind gusts from 7.1 km/h in 2022 to 6.5 km/h in 2023, with the average wind speed dropping from 2.8 km/h to 2.2 km/h. Solar radiation data were captured, showing a slight increase in 2023, with values rising from 230 W/m<sup>2</sup> in 2022 to 235 W/m<sup>2</sup> in 2023. Figure 3 illustrates the monthly rainfall and mean temperature variations during the 2022 and 2023 growing seasons.

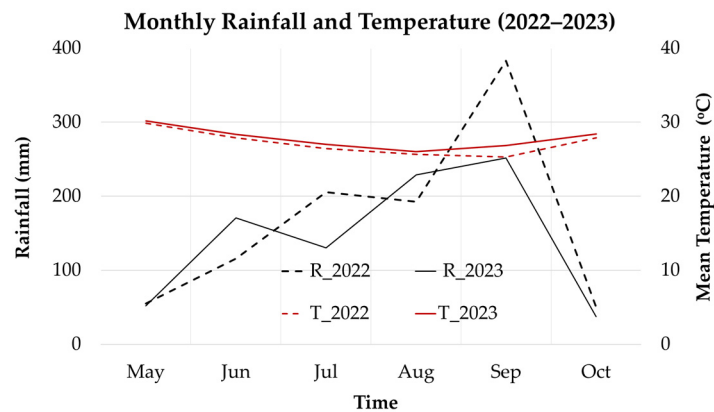


**Figure 3.** Rainfall and temperature variability: 2022 and 2023 rainy seasons in the study area (Nabdam).

The experiment focused on sorghum, widely favored by local farmers and recognized as the third most cultivated cereal in Ghana. The chosen variety, Kapaala white, endorsed by the regional research center, matures within 100 to 120 days. Sorghum cultivation in the area depends heavily on rainfall, with significant yield gaps observed. Actual yields have been reported to be 96.5% below the potential yield of  $2.0 \text{ Mt}\cdot\text{ha}^{-1}$  [38]. Planting typically begins in the first week of June, with flowering occurring in late August and harvesting concluding in early October, according to the agricultural calendar. Traditional compost fertilizer was uniformly applied across all study plots. Data collection spanned the years 2022 and 2023, with yield measurements taken from each plot, each covering an area of  $6 \text{ m} \times 6 \text{ m}$  and replicated three times.

#### 2.4. Soil Hydraulic Properties

Fifteen single-ring infiltration tests were conducted to estimate the saturated soil hydraulic conductivity ( $K_s$ ) using the Beerkan Estimation of Soil Transfer parameters through Infiltration Experiments (BEST) algorithm [39]. Eleven of these tests were performed in three stone bund plots located on a slope ranging from 6 to 10 degrees, with the steepest gradient observed in the upper bund. Four experiments were conducted in both the upper- and mid-bund plots, while three tests were carried out in the lower bund. Additionally, four tests were conducted in a control plot with a uniform 6-degree slope.

The BEST procedure enables the estimation of both the soil water retention curve (SWRC) and the hydraulic conductivity curve with minimal experimental data. Key inputs include particle-size distribution (PSD), dry soil bulk density, cumulative three-dimensional (3D) infiltration, and initial and final soil water content. The BEST method is based on the [39] model for the SWRC. It utilizes the [40] model for hydraulic conductivity, as expressed by the following equations:

$$K(Q) = K_s \left( \frac{\theta - \theta_r}{\theta_s - \theta_r} \right)^\eta \quad (1)$$

$$\eta = \frac{2}{m * n} + 3 + P \quad (2)$$

where  $K_s$  is the saturated soil hydraulic conductivity;  $\theta$  is the volumetric soil water content;  $\theta_s$  is the saturated soil volumetric water content;  $\theta_r$  is the residual volumetric soil water content;  $n$ ,  $m$ , and  $\eta$  are shape parameters; and  $P$  is a tortuosity parameter.

The determination of hydraulic parameters is performed in two stages. In the first stage, the SWRC shape parameters  $n$ ,  $m$ , and  $\eta$  are obtained from the PSD curve. An

analytical function is fitted to the PSD data (after excluding gravel fraction) and is given by the following equation:

$$F_D = \left[ 1 + \left( \frac{D_g}{D} \right)^{N_g} \right]^{-M_g} \quad (3)$$

where  $F_D$  is the cumulative particle mass fraction associated with particle diameter  $D$ ,  $D_g$  is a characteristic particle diameter, and  $N_g$  and  $M_g$  are shape parameters related by  $M_g = 1 - 1/N_g$ . The parameters  $n$  and  $m$  are linked to  $N_g$  and  $M_g$  by a relationship that involves soil porosity. The details of this calculation are provided by [39].

The remaining parameters are obtained from the infiltration experiment. Each test involved inserting a 15 cm diameter ring into the soil to a depth of at least 1 cm to prevent water loss from the soil surface. Infiltration tests were conducted under ponded conditions, where 150 mL of water was repeatedly added to the ring, and the time required for infiltration was recorded until a steady infiltration rate was achieved. Undisturbed soil samples were taken before and after the tests to measure dry bulk density and initial and final soil water content. Infiltration rates ( $f$ , mm/min) and cumulative infiltration ( $F$ , mm) were calculated based on the measured infiltration times and water volumes. The cumulative infiltration data were then used to derive  $K_s$  using the BEST slope algorithm [39].

### 2.5. NDVI Analysis

For the large-scale analysis, the NDVI data were acquired from Sentinel-2 satellite imagery, covering the Nabdam District from 1 January 2022 to 1 January 2024. The Sentinel-2 satellites, part of the European Union's Copernicus program (<https://dataspace.copernicus.eu/>, accessed on 8 September 2024), provide high-resolution imagery with a spatial resolution of up to 10 m and a revisit time of 5 days. This high frequency and fine resolution make Sentinel-2 data suitable for the long-term spatiotemporal analysis of vegetation dynamics, even in regions with relatively small and fragmented agricultural fields.

Twelve fields were selected to compare the effects of stone bunds on crop growth under rainfed conditions. Figure 3 illustrates a sample field polygon with stone bunds used for the NDVI data extraction in the study area (Nabdam, Ghana). These fields were identified through local surveys and were managed using the same crop type and agricultural practices. The geographic coordinates of these sites were registered, and additional information was collected from local partners. The control plots, without stone bunds, ranged in size from 2100 m<sup>2</sup> to 15,329 m<sup>2</sup>, collectively covering an area of 33,820 m<sup>2</sup>. The treatment plots, with stone bunds, ranged from 2200 m<sup>2</sup> to 20,876 m<sup>2</sup>, spanning a total area of 38,576 m<sup>2</sup>. The control plots were covered by 338 pixels, and the treatment plots were covered by approximately 386 pixels. Figure 4 illustrates the aerial view of the study plot with stone bunds, showing the field boundaries. The geographic coordinates are provided for spatial reference.

#### 2.5.1. NDVI Data Extraction and Processing

The NDVI data were obtained from the Copernicus Database portal (<https://dataspace.copernicus.eu/>, accessed on 8 September 2024). The Sentinel-2 Level-2A data were first filtered for cloud coverage, applying a threshold of 80%. Then, pixel-level cloud detection algorithms, specifically the Sentinel-2 Cloud Masking (s2cloudless) algorithm, were applied to mask out the pixels affected by clouds, shadows, and haze to further improve the data quality. Subsequently, the NDVI values for the filtered images corresponding to the selected acquisition dates were retrieved. The mean NDVI values for each field were retrieved from the cloud-free pixels on each acquisition date. The NDVI values for the selected fields were then downloaded and used directly for analysis. To improve the reliability of the analysis, NDVI values below 0.2 were excluded to eliminate non-vegetated areas. Finally, the daily NDVI values were obtained by linear interpolation between the available cloud-free images to create a continuous time series over the study period, ensuring that key vegetation growth stages were captured.

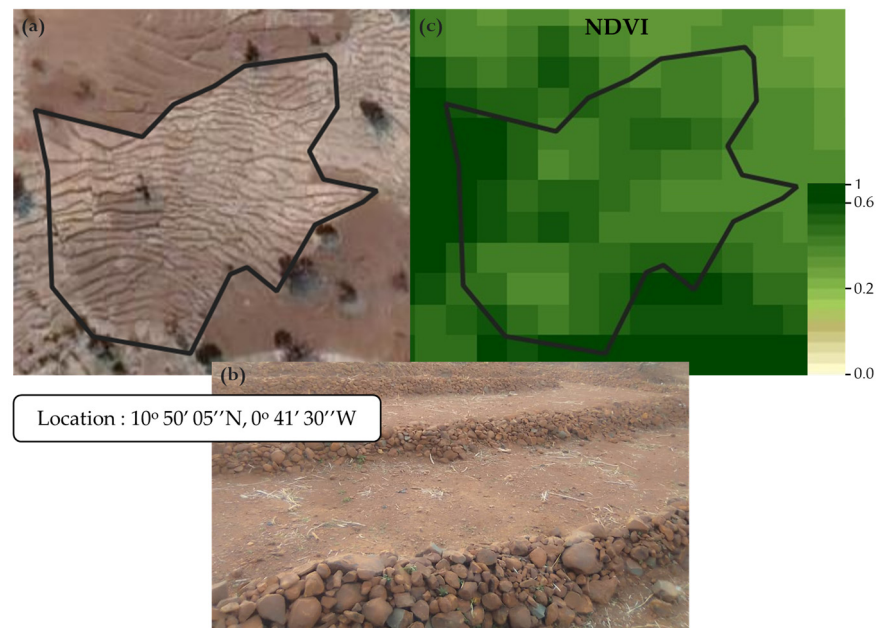


**Figure 4.** Sample stone bund polygon for NDVI data extraction in the study area (Nabdam, Ghana): Google Earth (a), actual image (b), and Sentinel 2 retrieved NDVI pixels for the 4 September 2023 (c).

### 2.5.2. NDVI Classification

In our methodology for analyzing the NDVI distributions, we categorized the NDVI data according to established threshold values. This classification approach is essential for interpreting the NDVI data effectively, allowing for us to distinguish between varying levels of vegetation vigor. The NDVI index ranges typically from  $-1$  to  $+1$ , with higher values indicating healthier and more vigorous vegetation. To facilitate our analysis, we defined specific threshold values to categorize the NDVI data (Table 2) according to literature sources [41–44]. By categorizing the NDVI values according to these thresholds, we can quantify and compare the vegetative cover in areas with stone bunds versus control areas, assessing the effectiveness of such land management practices in promoting vegetation health. This classification is valuable for mapping and monitoring changes in vegetation over time, providing a quantifiable measure of environmental impact.

**Table 2.** Vegetation classes and NDVI value.

NDVI Category	NDVI Range	Description
Low	$0.2 < \text{NDVI} < 0.3$	Sparse or stressed vegetation
Mid	$0.3 \leq \text{NDVI} < 0.5$	Moderate vegetation coverage
High	$\text{NDVI} \geq 0.5$	Dense and healthy vegetation

### 2.6. Statistical Analysis

To assess the effectiveness of stone bunds in enhancing soil moisture retention at different soil depths compared to control plots, we employed descriptive statistics, Pearson/Spearman correlation analysis with rainfall, and temporal trend analysis. Additionally, the percentage change in VWC at each soil depth between stone bunds and control plots was calculated using the following formula:

$$\% \Delta v_v = \left( \frac{V_{sb} - V_c}{V_c} \right) \times 100 \quad (4)$$

where  $\% \Delta v_v$  is the percent difference in VWC at each depth between the stone bunds ( $V_{sb}$ ) and control ( $V_c$ ) areas, providing a measure of the effectiveness of the stone bunds.

For non-normally distributed data, the non-parametric Wilcoxon rank sum test, also known as the Mann–Whitney U test, was used to compare two independent samples and determine if they come from the same distribution. It is particularly useful for comparing medians between two groups, i.e., stone bunds and control. The Wilcoxon rank sum test is defined as the following:

$$W = R_s - \frac{n_s(n_s + 1)}{2} \quad (5)$$

where  $R_s$  is the sum of the ranks and  $n_s$  is the number of observations in the stone bund sample. This test provides a  $p$ -value, and a  $p$ -value less than 0.05 typically indicates a statistically significant difference between the moisture content in the stone bund and control plots, leading to the rejection of the null hypothesis. The Wilcoxon rank sum test was performed using R, version 2024.04.2, a programming language and statistical software.

For the crop data, a two-way ANOVA (analysis of variance) was conducted to assess the effects of treatment (control vs. stone bunds) and year (2022 vs. 2023) on crop yield, including their interaction. The model included fixed effects for treatment and year and random effects for replication within each year. Significance was determined at  $p < 0.05$ . The data were structured with treatment and year as the main factors and crop yield as the response variable. The statistical model used was the following:

$$Y_{ijk} = \mu + \alpha_i + \beta_j + (\alpha\beta)_{ij} + \epsilon_{ijk} \quad (6)$$

where  $Y_{ijk}$  represents the yield for the  $k$ th replication in the  $i$ th treatment and  $j$ th year,  $\mu$  is the overall mean yield,  $\alpha_i$  is the effect of the  $i$ th treatment,  $\beta_j$  is the effect of the  $j$ th year,  $(\alpha\beta)_{ij}$  is the interaction effect between treatment and year, and  $\epsilon_{ijk}$  is the random error. The ANOVA was performed using the `aov` function in R, and the significance of the main effects and interaction was determined at the 0.05 significance level. The statistical analysis was conducted using RStudio version 2024.04.2 Build 764 (Posit Software, PBC), with R version 4.2.2 for documentation.

For the NDVI, the statistical analysis was performed using regression analysis to elucidate the relationship between the NDVI values and related variables, such as rainfall and soil moisture. Regression models were fitted to the dataset to quantitatively assess the impact of these factors on the NDVI. The significance of the coefficients was evaluated using statistical tests, including the  $t$ -statistic and  $p$ -value. Measures of model performance, such as R-squared and adjusted R-squared, were employed to gauge the explanatory power of the regression models, while the F-statistic provided insights into their overall significance.

The equations for simple and multiple linear regression are as follows:

For simple linear regression,

$$Y = \beta_0 + \beta_1 X_1 + \epsilon \quad (7)$$

For multiple linear regression,

$$Y = \beta_0 + \beta_1 X_1 + \beta_2 X_2 + \dots + \beta_p X_p + \epsilon \quad (8)$$

where  $X_1, X_2, \dots, X_p$  represent independent variables;  $\beta_1, \beta_2, \dots, \beta_p$  are the coefficients associated with each independent variable; and  $\epsilon$  represents the error term.

The methodology also included a residual analysis to validate the regression models and ensure the absence of systematic errors. Residual plots and tests for normality were conducted to assess the appropriateness of the regression assumptions and the accuracy of model predictions. Finally, smoothing techniques, such as moving averages, were employed to enhance the quality and reliability of the NDVI time-series data by mitigating noise and interpolating missing data points.

### 3. Results

#### 3.1. Soil Moisture Dynamics

The dataset analyzed in Figure 5, which includes in situ soil moisture and rainfall measurements taken at 15 min intervals, provides evidence of the effectiveness of stone bunds in regulating soil moisture, particularly under variable rainfall conditions. This analysis focuses on volumetric water content (VWC%) comparisons between stone bund and control plots, highlighting distinct moisture dynamics influenced by rainfall. The correlation coefficients between rainfall and soil moisture levels are 0.51 for the stone bund plots and 0.42 for the control plots. Figure 5a,b clearly show that stone bunds consistently maintain higher soil moisture levels, especially during periods of increased rainfall. Table 3 presents the statistics of soil moisture content in the stone bund and control areas. The stone bund areas sustained higher average VWC levels compared to the control areas, with notable increases at both 10 cm and 20 cm depths, quantitatively supporting the superior moisture retention capabilities of stone bunds. Specifically, the stone bund plots retained 21.33% more moisture than the control plots at 10 cm depth and 8.94% more at 20 cm depth over the entire study period. During the growing season of 2022, stone bunds retained 17.44% more moisture at 10 cm and 10.51% more at 20 cm. In 2023, these values increased to 22.99% and 23.70%, respectively.

**Table 3.** Statistics of rainfall (in mm/15 min) and soil moisture content (VWC, in %) at 10 cm and 20 cm depths in stone bund and control areas across three categories during the 2022 and 2023 rainy seasons as well as for all the study periods. SD stands for standard deviation.

		VWC Stone Bunds at 10 cm	VWC Control at 10 cm	VWC Stone Bunds at 20 cm	VWC Control at 20 cm
All study period	Maximum	50.3	42.3	54.6	49.3
	Mean	18.2	15	25.1	23.04
	SD	7.9	6.8	8.1	7.44
May–October 2022	Maximum	50.3	42.3	54.6	49.3
	Mean	22.02	18.75	31.23	28.26
	SD	6.43	5.9	9.7	8
May–October 2023	Maximum	45.5	39.7	47.2	39.8
	Mean	24.23	19.7	27.82	22.49
	SD	7.49	6.6	6.2	6.2

Despite a lower maximum rainfall of 22.9 mm in 2022, stone bunds helped achieve a soil moisture peak of 54.6 mm at 20 cm depth. Conversely, in 2023, a higher rainfall intensity of 26.4 mm resulted in a slightly lower moisture peak of 47.2 mm. Statistical validation using non-parametric tests, appropriate due to the non-normal distribution of the data, corroborates the hypothesis that stone bunds significantly improve soil moisture retention. The Wilcoxon rank sum test results at both 10 cm ( $W$  statistic: 225,254,  $p$ -value:  $1.979 \times 10^{-4}$ ) and 20 cm ( $W$  statistic: 244,776,  $p$ -value:  $1.053 \times 10^{-9}$ ) depths indicate that the differences in VWC between the stone bund and control areas are statistically significant. Figure 5a,b illustrate the temporal variations in soil moisture for both depths along with the corresponding rainfall events.

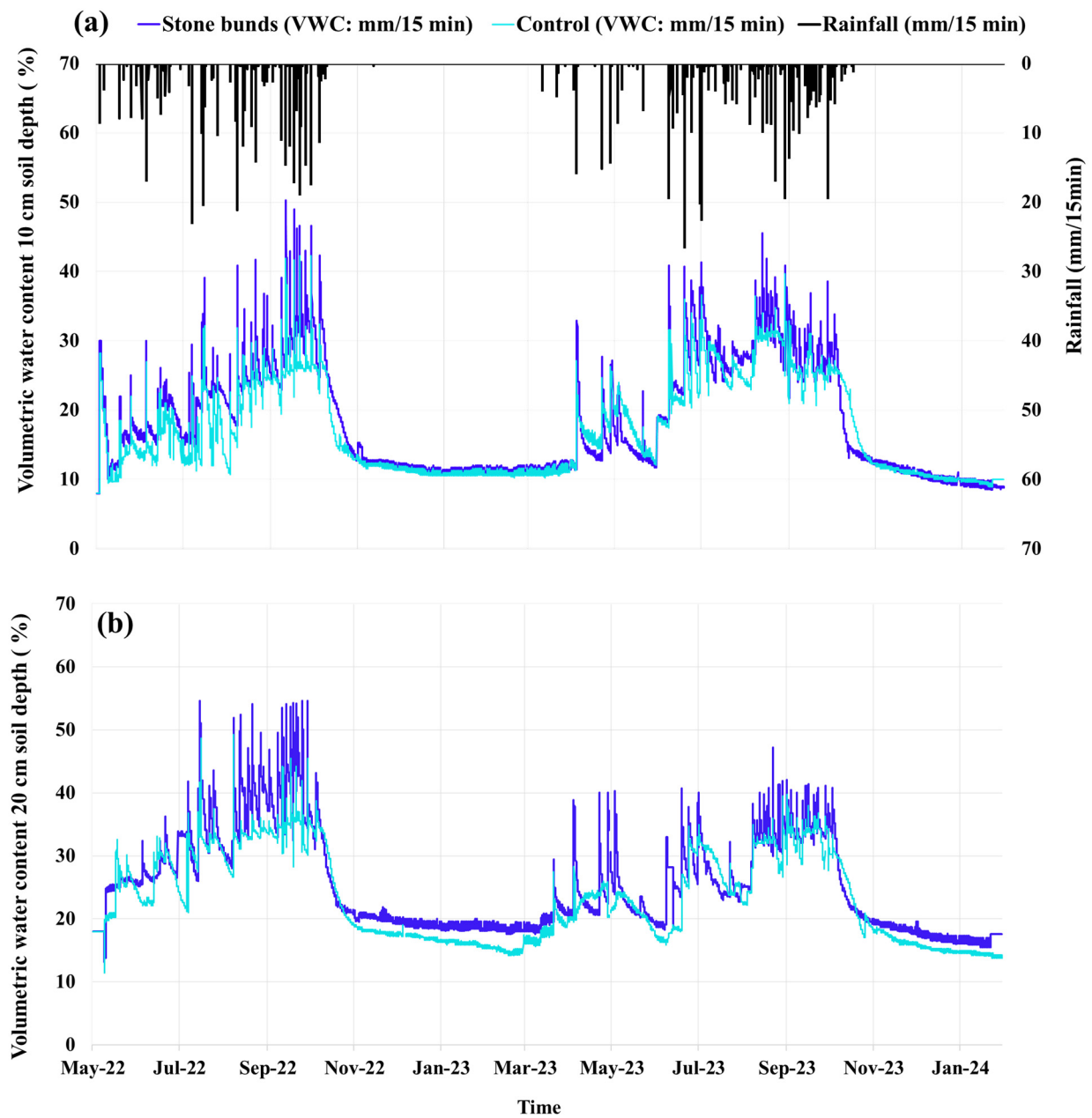


**Figure 5.** Observed time series of the rainfall and the soil water contents in the stone bunds and control areas at (a) 10 cm of soil depth; (b) 20 cm of soil depth. Data interval is 15 min.

### 3.2. Infiltration Rates and Hydraulic Conductivity

The mean instantaneous infiltration rate for the control plot was 6.2 mm/min compared to a higher rate of 8.7 mm/min for the stone bund plot. Additionally, the median infiltration rates were 4.8 mm/min for the control and 6.5 mm/min for the stone bunds, further demonstrating the enhanced water infiltration efficiency achieved with stone bunds. The mean cumulative infiltration was 95.2 mm for the control plot and 139.4 mm for the stone bund plots as shown in Figure 6. These results indicate that stone bunds could enhance soil permeability and water infiltration capacity compared to the control.

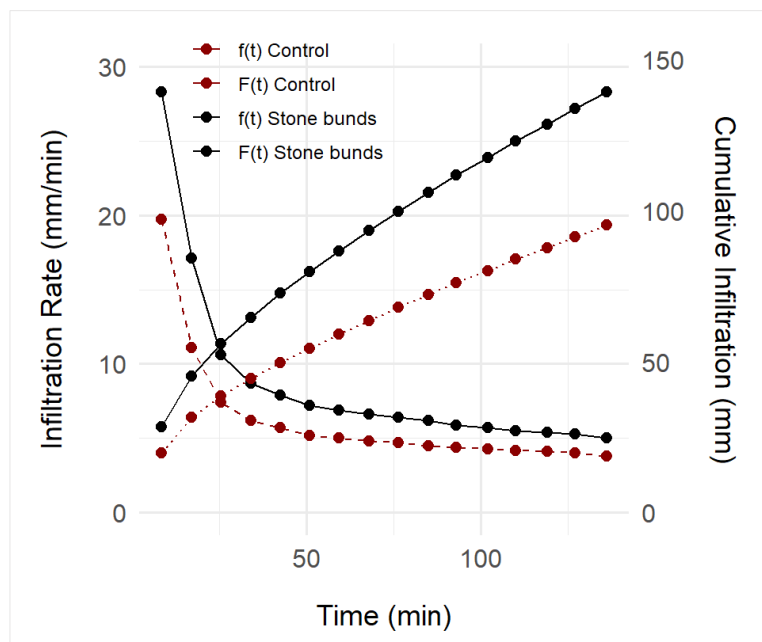


**Figure 6.** Cumulative infiltration (F(t)) and infiltration rate (f(t)) were measured in April 2022. The black lines (f(t)) represent the infiltration rates, whereas the brown lines (F(t)) illustrate the cumulative infiltration accumulated over time.

The mean soil’s saturated hydraulic conductivities ( $K_s$ ) were 1.732 mm/min and 1.185 mm/min in the stone bund and in the control, respectively. Table 4 provides detailed  $K_s$  values for the upper-, mid-, and lower-bund plots and the control plot. The three bunds showed higher mean  $K_s$  values compared to the control. Higher mean  $K_s$  values were found in the upper- and mid-stone bunds that had the highest slopes.

**Table 4.** Statistics for the saturated soil hydraulic conductivity ( $K_s$ ) determined in different plot locations during April 2022.

Plot	Infiltration Tests	$K_s$ Min (mm/min)	$K_s$ Max (mm/min)	$K_s$ Mean (mm/min)	Standard Dev (mm/min)
Upper-Bund	4	0.992	3.232	1.654	0.917
Mid-Bund	4	0.802	2.853	2.032	0.858
Lower-Bund	3	0.858	2.047	1.435	0.486
Control	4	0.834	1.832	1.185	0.399

A temporal analysis of rainfall recorded at 15 min intervals in conjunction with the saturated hydraulic conductivity ( $K_s$ ) offers valuable insights into the likelihood of surface runoff occurrence. This analysis assumes a uniform rainfall rate within the 15 min data acquisition intervals. During the rainy seasons of 2022 and 2023, eleven 15 min rainfall observations in the control plot exceeded the average  $K_s$  value, indicating the potential for surface runoff. In contrast, only one rainfall event in the plots with stone bunds surpassed the mean  $K_s$  value. The observed peaks in soil moisture within the stone bund plots suggest a higher rate of infiltration, providing a more accurate reflection of the rainfall recorded at these intervals. This variation illustrates that soil moisture responses are better correlated with rainfall events, especially since rainfall is not uniformly distributed over the 15 min intervals. The control plot, lacking these pronounced peaks, struggles to absorb the intensity of rainfall, leading to increased runoff.

### 3.3. NDVI Analysis and Vegetation Response to Stone Bunds

The NDVI analysis over the growing seasons of 2022 and 2023 reveals that stone bunds consistently result in higher NDVI values compared to the control plots, indicating better vegetation health and growth. During the peak growth from mid-August to mid-September, the NDVI values in the stone bund fields reached 0.61, while the control fields recorded lower values of 0.52 in 2022 and 0.48 in 2023. Figure 7 illustrates the dynamics of the mean daily NDVI values from multiple plots under different management practices (with and without stone bunds) across the 2022–2023 growing seasons. The analysis shows that, in 2022, the stone bund fields exhibited higher NDVI values from sowing to mid-season (approximately up to day of year 230), attributed to favorable conditions, like higher rainfall and better soil moisture. From DOY 150 to DOY 200, the plots with stone bunds of 2023 were higher than the 2023 control plots and similar to the 2022 control plots. After DOY 200, in 2023, the plot with stone bunds maintained higher NDVI levels than the control plots of 2022, despite the lower rainfall, and reached similar values to the stone bund plot of 2022 near mid-season. The decline in NDVI values towards the end of the season corresponds to the physiological maturation and harvesting phases of the crops. Figure 5 illustrates the temporal dynamics of the mean daily normalized difference vegetation index (NDVI) values for two consecutive years across different agricultural stages.

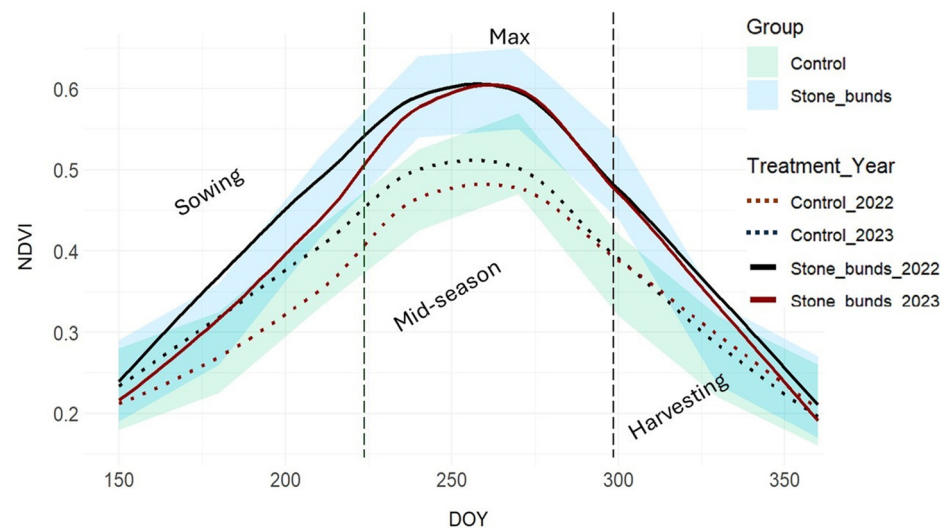


**Figure 7.** Temporal dynamics of mean daily normalized difference vegetation index (NDVI) values for two consecutive years across different agricultural stages, marked by days of the year (DOY). The shaded regions denote the confidence intervals, providing an estimate of variability around the mean and the vertical dashed line separates the cropping season (Sowing, Mid-season and Harvesting periods).

A pixel-based spatiotemporal analysis of the NDVI distributions, as illustrated in Figure 8, during the rainy periods (May to October) reveals significant differences of vegetation vigor between the areas with and without stone bunds. The stone bund areas exhibited a higher percentage of high NDVI (24%) compared to the control areas (9.2%).

Statistical analysis reveals significant effects of both treatment (presence or absence of stone bunds) and location on the NDVI values, as shown in Table 5. The presence of stone bunds significantly increased the NDVI ( $p < 0.001$ ), indicating their positive impact on vegetation vigor. The location also showed a significant effect on the NDVI ( $p < 0.001$ ), suggesting spatial variability in vegetation response across different sites. Notably, the absence of a significant interaction effect between treatment and location suggests that the beneficial effects of stone bunds are consistent across various locations.

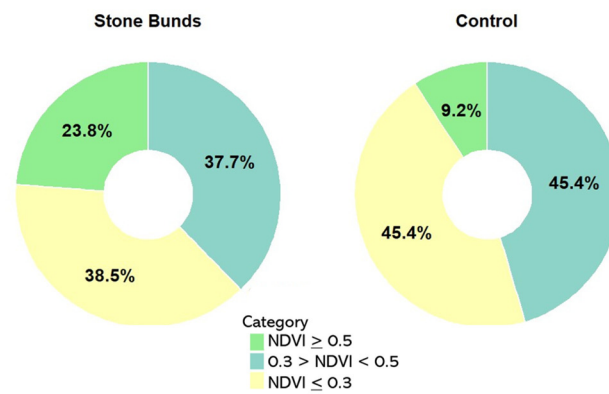


**Figure 8.** NDVI pixel distribution over the two seasons (2022–2023).

**Table 5.** ANOVA results for treatment and location effects on NDVI.

	Df	Sum Sq	Mean Sq	F-Value	Pr (>F)	Significance
Treatment	1	0.232	0.2322	17.262	$3.79 \times 10^{-5}$	***
Location	5	0.318	0.0636	4.729	0.000309	***
Rainfall	1	2.39	2.3901	177.678	$<2 \times 10^{-16}$	***
Treatment: Location	5	0.033	0.0066	0.492	0.782596	No
Treatment: Rainfall	1	0.062	0.0618	4.596	0.032492	*
Residuals	26	0.22	0.01			

Significance. codes: 0 '\*\*\*' 0.001 '\*\*' 0.05.

Further analysis of the interaction between rainfall and the NDVI reveals significant impacts, particularly in regions with stone bunds. In these areas, the correlation coefficient between rainfall and the NDVI is 0.68, indicating a robust positive relationship, compared to a moderate positive correlation of 0.57 in areas without stone bunds. Regression analysis further elucidates this relationship. In the presence of stone bunds, the multiple R is 0.69, with an  $R^2$  of 0.48, implying that 48% of the NDVI variation can be attributed to rainfall. This association is statistically significant, supported by an F-statistic and a  $p$ -value. Conversely, in the absence of stone bunds, the multiple R is 0.67, and the  $R^2$  indicates that 44% of the NDVI variation is explained by rainfall, supported by an F-statistic of 331.2 and a  $p$ -value of  $8.53644 \times 10^{-55}$ .

### 3.4. Crop Yield Response

A statistical analysis was conducted to examine the effects of treatment type (control vs. stone bunds) and year (2022 vs. 2023) on crop yield, including their interaction. The analysis revealed a statistically significant main effect of treatment on yield,  $F_{(1,10)} = 479.39$ ,  $p < 0.001$ , indicating that the use of stone bunds significantly increased crop yields compared to the control treatment. Specifically, the mean yields were higher by 38.1% in 2022 and 32.05% in 2023 compared to the control. Additionally, there was a significant main effect of year on yield,  $F_{(1,5)} = 13.69$ ,  $p = 0.014$ , suggesting that crop yields differed significantly between the two years, potentially due to varying environmental conditions or other temporal factors. Figure 9 illustrates the mean yield of sorghum under stone bunds compared to the control plot over the two years. The mean yields were higher in 2022 than in 2023 for both treatments. Despite lower overall rainfall in 2023, the timing, distribution, and amount of rainfall likely contributed to the yield reduction. The interaction between treatment and year was not significant,  $F_{(1,10)} = 0.001$ ,  $p = 0.975$ , indicating that the increase in yield due to the stone bunds treatment was consistent across both years.

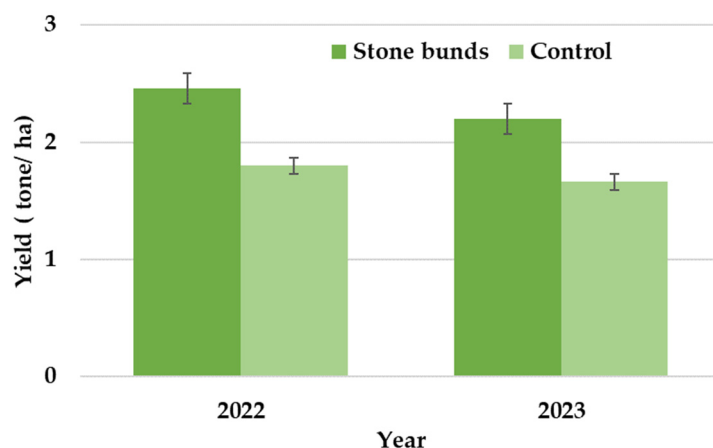


**Figure 9.** Mean yield of sorghum (Kapaala White) under stone bunds and control plot over the two years.

#### 4. Discussion

The decrease in rainfall in 2023, from 1002 mm in 2022 to 871 mm, led to lower soil moisture levels, impacting crop growth and water availability. Abdisa, Mamo Diga, and Regassa Tolessa [45] and Tolosa, Dadi, Mirkena, Erena, and Liban [46] found that over 75% of the variability in sorghum yields in Ethiopia is attributable to fluctuations in rainfall and temperature. The infiltration tests showed the benefits of using stone bunds for improving soil characteristics for more productive rainfed agriculture. The higher mean infiltration rate observed in the stone bunds compared to control plots indicates an improved infiltration capacity. The slightly higher saturated hydraulic conductivity ( $K_s$ ) evaluated for the stone bunds indicates soil conditions that facilitate water movement through the soil profile, underscoring the potential of stone bunds to enhance water retention and reduce surface. The temporal analysis of  $K_s$  in relation to the 15 min rainfall during the rainy seasons suggests that stone bunds can mitigate the risks of infiltration excess consequent to heavy rainfall events [47]. The observed soil moisture dynamics further demonstrate the effectiveness of stone bunds in enhancing rainfed agricultural resilience. The stone bunds consistently maintained higher soil moisture levels with respect to the control plot, especially during periods of increased rainfall, mirroring the findings from Singh, K., Emanuel, McGlynn, and Miniati [29,48]. The higher mean VWC observed in the stone bund plots over the study period reflects significant improvements in moisture retention. Additionally, the greater VWC at deeper soil layers in these plots can be attributed to the enhanced infiltration and water retention capacity associated with stone bunds. The exceptionally low  $p$ -values, well below the conventional threshold of 0.05, confirm that stone bunds enhance soil moisture retention more effectively at both observed soil depths, underscoring their potential as a valuable strategy for sustainable agricultural practices in water-limited environments. These findings highlight the positive impact of stone bunds in optimizing soil moisture during reduced rainfall periods (Kirkby, M.J. and R.P.C. [49]), which is essential for sustainable agriculture in challenging environmental conditions.

The effectiveness of stone bunds in managing soil moisture is evident from our intermediate data. In 2022, despite a lower maximum rainfall, stone bunds achieved the highest soil moisture peak at a 20 cm depth. Conversely, in 2023, a higher rainfall intensity of 26.4 mm resulted in a lower moisture peak. This highlights the importance of considering slope and rainfall intensity when optimizing stone bunds to capture and retain more moisture. Adapting the design of stone bunds to the local conditions is essential for maximizing their benefits. Proper maintenance and strategic design of stone bunds are crucial for optimizing soil moisture retention and minimizing erosion, particularly in regions with variable rainfall patterns [29,50]. The effectiveness of stone bunds is significantly enhanced by tailoring their height and ensuring their structural integrity to accommodate different rainfall intensities [14,34,51]. This approach not only prevents waterlogging during intense

rainfall events but also ensures adequate moisture availability during drier periods. Regular monitoring and community involvement in maintaining these structures are essential for sustaining their benefits, making agricultural systems more resilient and productive in the face of climatic challenges.

The NDVI analysis conducted during the growing seasons of 2022 and 2023 reveals that stone bunds consistently yield higher NDVI values than control plots. High NDVI values are typically associated with improved crop health and biomass, directly correlating with increased yields [52,53]. The enhanced vegetation cover in areas with stone bunds indicates that these structures create optimal growth conditions for sorghum, particularly during the growth season when the crop's water demands are highest, supporting the findings from Liu, Li, Li, and Motesharrei [54] and Mando and Stroosnijder [55]. However, increased vegetation vigor does not always translate to higher yields, as rainfall during non-critical growth stages can enhance the NDVI without significantly benefiting grain filling [56–58].

In this study, the improved vegetation health likely contributed to increased sorghum yields, emphasizing the effectiveness of stone bunds as a soil and water conservation strategy in rainfed agricultural systems. Specifically, the average yields were consistently higher in the stone bund plots compared to the control plots, aligning with prior research that highlights the positive impact of stone bunds on agricultural productivity [16,29]. Interestingly, the mean yields were higher in 2022 than in 2023 for both treatments, likely due to reduced rainfall in 2023 creating less favorable conditions for sorghum growth and yield. Nonetheless, the plots with stone bunds in 2023 still outperformed the control plots from 2022, which had received more rainfall, indicating that stone bunds increase the resilience of this rainfed agriculture to drought periods.

This finding is particularly significant because better moisture management is critical for maintaining crop health and increasing yields, especially given the increasingly erratic weather conditions affecting rainfed agricultural systems. Rainfed agriculture is highly susceptible to changes in rainfall patterns and intensity, leading to significant agricultural losses due to both drought and excessive rainfall disrupting crop growth cycles [59]. The changing climate further complicates water management, with intense rainfall events causing rapid runoff and decreased water availability for crops [60]. Additionally, regions like the Upper East Region of Ghana have recently experienced a shift toward less frequent but more intense rainfall events [61]. This shift poses significant threats to rainfed agriculture, as increased rainfall intensity leads to heightened runoff and soil erosion, while less distributed rainfall results in insufficient water for crops during critical growing periods. Tolosa, Dadi [46] underscored the importance of rainfall distribution, showing strong correlations between sorghum yields and the number of rainy days throughout the growing season.

The consistency of results in soil hydraulic conductivity, infiltration rates, soil moisture dynamics, the NDVI, and yield across this field study suggests that stone bunds are a beneficial agricultural practice capable of enhancing rainfed agriculture and crop yields despite annual variations. Our results are in line with other studies in different African drylands, which have demonstrated that stone bunds can significantly enhance sorghum yields by improving soil fertility and moisture availability [62,63] or by enhancing soil water retention and reducing runoff [64]. These results are particularly important for developing sustainable agricultural strategies that can withstand yearly fluctuations, ensuring more predictable and stable improvements in crop productivity. However, as this analysis is based on only two years of data and limited locations, further research over a more extended period is recommended to confirm these findings and ensure their generalizability across different environmental conditions and periods. Overall, the results demonstrate the significant agronomic benefits of implementing stone bunds in crop production, leading to higher yields compared to traditional methods.

## 5. Conclusions

Combining in situ soil moisture measurements, remote sensing data (NDVI), and yield data, this study provides a thorough assessment of the effectiveness of stone bunds in semi-arid regions of Ghana's Upper East Region. By improving surface infiltration and soil moisture and increasing crop yields, stone bunds effectively address the challenges posed by climate variability and changing rainfall patterns. These findings highlight the significance of integrating stone bunds into agricultural practices to promote sustainable and resilient crop production.

The consistent positive effects observed across multiple metrics and years affirm stone bunds as a valuable tool for enhancing agricultural productivity, food security, and the sustainability of rainfed agriculture. These results advocate for more sustainable farming practices and improved food security in semi-arid regions. For policymakers and practitioners, the findings underscore the need to promote stone bunds as part of integrated soil and water management strategies. Implementing training programs and providing support for farmers in the construction and maintenance of stone bunds can facilitate widespread adoption and maximize their impact on agricultural productivity.

While this study provides evidence of the benefits of stone bunds, future research should explore their long-term impacts and integration with other sustainable farming practices. Conducting longitudinal studies over multiple growing seasons and extended periods is recommended to validate these findings and assess their applicability across diverse environmental conditions and timelines.

**Author Contributions:** H.A., M.L.T. and M.P. developed the research methodology framework and performed the analysis. The manuscript was written by H.A., M.L.T. and M.P. and reviewed by all authors. M.L.T., J.A.-D., R.A., P.A.A. and G.M. acquired and provided the field data, which were processed by M.L.T. Team coordination and supervision were overseen by G.S., J.M.K. and A.C. All authors have read and agreed to the published version of the manuscript.

**Funding:** This research was funded by the EU Horizon 2020 EWA-BELT project [GA 862848] "Linking East and West African farming systems experience into a BELT of sustainable intensification" coordinated by the Desertification Research Centre of the University of Sassari.

**Data Availability Statement:** Data will be made available on request.

**Acknowledgments:** The authors would like to acknowledge the EWA\_BELT European Union's Horizon 2020 research and innovation program under grant agreement No 862848 project and University of Sassari Department of Agriculture of Sassari, Desertification Research Centre (NRD).

**Conflicts of Interest:** Author James Mantent Kombiok, employed by Kundok Development Consult (KDC). The remaining authors declare that the research was conducted in the absence of any commercial or financial relationships that could be construed as a potential conflict of interest.

## References

1. Amponsem, J. Climate Change: Drought Hits Ghana's Second Farming Season. 2015. Available online: <https://www.modernghana.com/news/641431/climate-change-drought-hits-ghanas-second-farming-season.html> (accessed on 30 July 2024).
2. FAO. Ghana at a Glance. 2024. Available online: <https://www.fao.org/ghana/fao-in-ghana/ghana-at-a-glance/en/> (accessed on 31 May 2024).
3. Quinton, J. *Desertification, Land Degradation and Sustainability: Paradigms, Processes, Principles and Policies*; Imeson, A., Ed.; John Wiley & Sons Ltd.: Chichester, UK, 2012. [CrossRef]
4. Breman, H. Desertification control, the West African case; prevention is better than cure. *Biotropica* **1992**, *24*, 328–334. [CrossRef]
5. Darkoh, M.B. Desertification in Africa. *J. East. Afr. Res. Dev.* **1989**, *19*, 1–50.
6. Warren, A.; Batterbury, S.; Osbahr, H. Soil erosion in the West African Sahel: A review and an application of a "local political ecology" approach in South West Niger. *Glob. Environ. Chang.* **2001**, *11*, 79–95. [CrossRef]
7. Yirdaw, E.; Tigabu, M.; Monge, A. Rehabilitation of degraded dryland ecosystems—Review. *Silva Fenn.* **2017**, *51*, 1673. [CrossRef]
8. Dang, H.L.; Li, E.; Nuberg, I.; Bruwer, J. Factors influencing the adaptation of farmers in response to climate change: A review. *Clim. Dev.* **2019**, *11*, 765–774. [CrossRef]
9. Tefera, M.L.; Seddaiu, G.; Carletti, A. Traditional In Situ Water Harvesting Practices and Agricultural Sustainability in Sub-Saharan Africa—A Meta-Analysis. *Sustainability* **2024**, *16*, 6427. [CrossRef]

10. Tefera, M.L.; Carletti, A.; Altea, L.; Rizzu, M.; Migheli, Q.; Seddaiu, G. Land degradation and the upper hand of sustainable agricultural intensification in sub-Saharan Africa—A systematic review. *J. Agric. Rural Dev. Trop. Subtrop.* **2014**, *125*, 63–83. [[CrossRef](#)]
11. Hossini, H.; Karimi, H.; Mustafa, Y.T.; Al-Quraishi, A.M.F. Role of Effective Factors on Soil Erosion and Land Degradation: A Review. In *Environmental Degradation in Asia*; Earth and Environmental Sciences Library; Springer: Cham, Switzerland, 2022; pp. 221–235. [[CrossRef](#)]
12. Li, H.; Zhu, H.; Liang, C.; Wei, X.; Yao, Y. Soil erosion significantly decreases aggregate-associated OC and N in agricultural soils of Northeast China. *Agric. Ecosyst. Environ.* **2022**, *323*, 107677. [[CrossRef](#)]
13. Indoria, A.K.; Sharma, K.L.; Reddy, K.S. Hydraulic properties of soil under warming climate. In *Climate Change and Soil Interactions*; Elsevier: Amsterdam, The Netherlands, 2020; pp. 473–508.
14. Taye, G.; Poesen, J.; Vanmaercke, M.; van Wesemael, B.; Martens, L.; Teka, D.; Nyssen, J.; Deckers, J.; Vanacker, V.; Haregeweyn, N.; et al. Evolution of the effectiveness of stone bunds and trenches in reducing runoff and soil loss in the semi-arid Ethiopian highlands. *Z. Geomorphol.* **2015**, *59*, 477–493. [[CrossRef](#)]
15. Taye, G.; Tesfaye, S.; Van Parijs, I.; Poesen, J.; Vanmaercke, M.; van Wesemael, B.; Guyassaa, E.; Nyssen, J.; Deckers, J.; Haregeweyn, N. Impact of soil and water conservation structures on the spatial variability of topsoil moisture content and crop productivity in semi-arid Ethiopia. *Soil Tillage Res.* **2024**, *238*, 105998. [[CrossRef](#)]
16. Zougmore, R.; Jalloh, A.; Tioro, A. Climate-smart soil water and nutrient management options in semiarid West Africa: A review of evidence and analysis of stone bunds and zaï techniques. *Agric. Food Secur.* **2014**, *3*, 16. [[CrossRef](#)]
17. Surendran, U.; Nagakumar, K.C.V.; Samuel, M.P. Remote Sensing in Precision Agriculture. In *Digital Agriculture*; Springer International Publishing: Cham, Switzerland, 2024; pp. 201–223.
18. Rekha, B.U.; Desai, V.V.; Ajawan, P.S.; Jha, S.K. Remote Sensing Technology and Applications in Agriculture. In Proceedings of the International Conference on Computational Techniques, Belgaum, India, 21–22 December 2018; pp. 193–197.
19. Kumar, S.; Meena, R.S.; Sheoran, S.; Jangir, C.K.; Jhariya, M.K.; Banerjee, A.; Raj, A. Remote sensing for agriculture and resource management. In *Natural Resources Conservation and Advances for Sustainability*; Elsevier: Amsterdam, The Netherlands, 2022; pp. 91–135.
20. Zhang, H.; Chang, J.; Zhang, L.; Wang, Y.; Li, Y.; Wang, X. NDVI dynamic changes and their relationship with meteorological factors and soil moisture. *Environ. Earth Sci.* **2018**, *77*, 582. [[CrossRef](#)]
21. Wang, Y.W. Sustainable agricultural practices: Energy inputs and outputs, pesticide, fertilizer and greenhouse gas management. *Asia Pac. J. Clin. Nutr.* **2009**, *18*, 498–500.
22. Felegari, S.; Sharifi, A.; Moravej, K.; Golchin, A.; Tariq, A. Investigation of the Relationship Between NDVI Index, Soil Moisture, and Precipitation Data Using Satellite Images. In *Sustainable Agriculture Systems and Technologies*; Wiley: Hoboken, NJ, USA, 2022; pp. 314–325. [[CrossRef](#)]
23. Ding, Y.; He, X.; Zhou, Z.; Hu, J.; Cai, H.; Wang, X.; Li, L.; Xu, J.; Shi, H. Response of vegetation to drought and yield monitoring based on NDVI and SIF. *Catena* **2022**, *219*, 106328. [[CrossRef](#)]
24. Ihuoma, S.O.; Madramootoo, C.A.; Kalacska, M. Integration of satellite imagery and in situ soil moisture data for estimating irrigation water requirements. *Int. J. Appl. Earth Obs. Geoinf.* **2021**, *102*, 102396. [[CrossRef](#)]
25. Chanev, M.; Kamenova, I.; Filchev, L. Remote Sensing Monitoring of Water Productivity in Agricultural Crops: A Review. In *River Conservation and Water Resource Management*; Advances in Geographical and Environmental Sciences; Springer: Singapore, 2023; pp. 17–26. [[CrossRef](#)]
26. Singh, R. Bunds. In *Soil and Water Conservation Structures Design*; Water Science and Technology Library; Springer: Singapore, 2023; pp. 95–119. [[CrossRef](#)]
27. Naazie, G.K.; Dakyaga, F.; Derbile, E.K. Agro-ecological intensification for climate change adaptation: Tales on soil and water management practices of smallholder farmers in rural Ghana. *Discov. Sustain.* **2023**, *4*, 27. [[CrossRef](#)]
28. Meresa, M.; Tadesse, M.; Zeray, N. Effect of soil and water conservation structures on smallholder farmers' livelihood: Wenago district, Southern Ethiopia. *Cogent Soc. Sci.* **2023**, *9*, 2272305. [[CrossRef](#)]
29. Alemayehu, A.A.; Getu, L.A.; Addis, H.K.; Tejada Moral, K. Impacts of stone bunds on selected soil properties and crop yield in Gumara-Maksegnit watershed Northern Ethiopia. *Cogent Food Agric.* **2020**, *6*, 1785777. [[CrossRef](#)]
30. Barry, B.; Olaleye, A.O.; Zougmore, R.; Fatondji, D. *Rainwater Harvesting Technologies in the Sahelian Zone of West Africa and the Potential for Outscaling*; IWMI: Colombo, Sri Lanka, 2008; p. 40.
31. Wolka, K.; Moges, A.; Yimer, F. Effects of level soil bunds and stone bunds on soil properties and its implications for crop production: The case of Bokole watershed, Dawuro zone, Southern Ethiopia. *Agric. Sci.* **2011**, *2*, 357–363. [[CrossRef](#)]
32. Wolka, K.; Mulder, J.; Biazin, B. Effects of soil and water conservation techniques on crop yield, runoff and soil loss in Sub-Saharan Africa: A review. *Agric. Water Manag.* **2018**, *207*, 67–79. [[CrossRef](#)]
33. Abi, M.; Kessler, A.; Oosterveer, P.; Tolossa, D. Understanding the Spontaneous Spreading of Stone Bunds in Ethiopia: Implications for Sustainable Land Management. *Sustainability* **2018**, *10*, 2666. [[CrossRef](#)]
34. Nyssen, J.; Poesen, J.; Gebremichael, D.; Vancampenhout, K.; D'aes, M.; Yihdego, G.; Govers, G.; Leirs, H.; Moeyersons, J.; Naudts, J.; et al. Interdisciplinary on-site evaluation of stone bunds to control soil erosion on cropland in Northern Ethiopia. *Soil Tillage Res.* **2007**, *94*, 151–163. [[CrossRef](#)]

35. Sultan, D.; Tsunekawa, A.; Haregeweyn, N.; Adgo, E.; Tsubo, M.; Meshesha, D.T.; Masunaga, T.; Aklog, D.; Fenta, A.A.; Ebabu, K. Impact of Soil and Water Conservation Interventions on Watershed Runoff Response in a Tropical Humid Highland of Ethiopia. *Environ. Manag.* **2018**, *61*, 860–874. [[CrossRef](#)] [[PubMed](#)]
36. Blake, G.R.; Hartge, K.H. Bulk Density. In *Methods of Soil Analysis*; Klute, A., Ed.; SSSA Book Series; Soil Science Society of America (SSSA): Madison, WI, USA, 1986; pp. 363–375. [[CrossRef](#)]
37. USDA. *Soil Taxonomy: A Basic System of Soil Classification for Making and Interpreting Soil Surveys*, 2nd ed.; USDA-Natural Resources Conservation Service. U.S. Government Printing Office: Washington, DC, USA, 1999.
38. AfricaagMedia. Ghana: Sorghum. 15 September 2021. Available online: <http://www.agricinafrica.com/2021/09/ghana-sorghum.html> (accessed on 27 May 2024).
39. Van Genuchten, M.T. A closed-form equation for predicting the hydraulic conductivity of unsaturated soils. *Soil Sci. Soc. Am. J.* **1980**, *44*, 892–898. [[CrossRef](#)]
40. Brooks, R.H.; Corey, A.T. *Hydrology Papers*; Colorado State University: Fort Collins, CO, USA, 1964.
41. Angulo-Jaramillo, R.; Bagarello, V.; Di Prima, S.; Gosset, A.; Iovino, M.; Lassabatere, L. Beerkan Estimation of Soil Transfer parameters (BEST) across soils and scales. *J. Hydrol.* **2019**, *576*, 239–261. [[CrossRef](#)]
42. Aranguren, M.; Castellón, A.; Aizpurua, A. Wheat Yield Estimation with NDVI Values Using a Proximal Sensing Tool. *Remote Sens.* **2020**, *12*, 2749. [[CrossRef](#)]
43. Dalezios, N.R.; Domenikiotis, C.; Loukas, A.; Tzortzios, S.T.; Kalaitzidis, C. Cotton yield estimation based on NOAA/AVHRR produced NDVI. *Phys. Chem. Earth Part B Hydrol. Ocean. Atmos.* **2001**, *26*, 247–251. [[CrossRef](#)]
44. Lee, G.; Kim, G.; Min, G.; Kim, M.; Jung, S.; Hwang, J.; Cho, S. Vegetation Classification in Urban Areas by Combining UAV-Based NDVI and Thermal Infrared Image. *Appl. Sci.* **2022**, *13*, 515. [[CrossRef](#)]
45. Abdisa, B.T.; Mamo Diga, G.; Regassa Tolessa, A. Impact of climate variability on rain-fed maize and sorghum yield among smallholder farmers. *Cogent Food Agric.* **2022**, *8*, 2057656. [[CrossRef](#)]
46. Tolosa, A.A.; Dadi, D.K.; Mirkena, L.W.; Erena, Z.B.; Liban, F.M. Impacts of Climate Variability and Change on Sorghum Crop Yield in the Babile District of Eastern Ethiopia. *Climate* **2023**, *11*, 99. [[CrossRef](#)]
47. Horton, R.E. An Approach Toward a Physical Interpretation of Infiltration-Capacity. *Soil Sci. Soc. Am. J.* **1941**, *5*, 399–417. [[CrossRef](#)]
48. Singh, N.K.; Emanuel, R.E.; McGlynn, B.L.; Miniati, C.F. Soil Moisture Responses to Rainfall: Implications for Runoff Generation. *Water Resour. Res.* **2021**, *57*, e2020WR028827. [[CrossRef](#)]
49. Kirkby, M.J.; Morgan, R.P.C. Soil Erosion. In *Journal of Hydrology*; J.W. Sons: Chichester, UK, 1982; Volume 55.
50. Klik, A.; Schürz, C.; Strohmeyer, S.; Demelash Melaku, N.; Ziadat, F.; Schwen, A.; Zucca, C. Impact of stone bunds on temporal and spatial variability of soil physical properties: A field study from northern Ethiopia. *Land Degrad. Dev.* **2018**, *29*, 585–595. [[CrossRef](#)]
51. Gebremichael, D.; Nyssen, J.; Poesen, J.; Deckers, J.; Haile, M.; Govers, G.; Moeyersons, J. Effectiveness of stone bunds in controlling soil erosion on cropland in the Tigray Highlands, northern Ethiopia. *Soil Use Manag.* **2005**, *21*, 287–297. [[CrossRef](#)]
52. Bannari, A.; Morin, D.; Bonn, F.; Huete, A.R. A review of vegetation indices. *Remote Sens. Rev.* **1995**, *13*, 95–120. [[CrossRef](#)]
53. Wiegand, C.L.; Richardson, A.J.; Escobar, D.E.; Gerbermann, A.H. Vegetation indices in crop assessments. *Remote Sens. Environ.* **1991**, *35*, 105–119. [[CrossRef](#)]
54. Liu, Y.; Li, Y.; Li, S.; Motescharrei, S. Spatial and Temporal Patterns of Global NDVI Trends: Correlations with Climate and Human Factors. *Remote Sens.* **2015**, *7*, 13233–13250. [[CrossRef](#)]
55. Mando, A.; Stroosnijder, L. The biological and physical role of mulch in the rehabilitation of crusted soil in the Sahel. *Soil Use Manag.* **2006**, *15*, 123–127. [[CrossRef](#)]
56. Akinseye, F.M.; Ajeigbe, H.A.; Traore, P.C.S.; Agele, S.O.; Zemadim, B.; Whitbread, A. Improving sorghum productivity under changing climatic conditions: A modelling approach. *Field Crops Res.* **2020**, *246*, 107685. [[CrossRef](#)]
57. Katerji, N.; Mastrorilli, M. Water Use Efficiency of Cultivated Crops. In *Encyclopedia of Life Sciences*; Wiley: Hoboken, NJ, USA, 2014. [[CrossRef](#)]
58. Wakjira, M.T.; Peleg, N.; Anghileri, D.; Molnar, D.; Alamirew, T.; Six, J.; Molnar, P. Rainfall seasonality and timing: Implications for cereal crop production in Ethiopia. *Agric. For. Meteorol.* **2021**, *310*, 108633. [[CrossRef](#)]
59. Liaqat, W.; Altaf, M.T.; Barutçular, C.; Mohamed, H.I.; Ahmad, H.; Jan, M.F.; Khan, E.H. Sorghum: A Star Crop to Combat Abiotic Stresses, Food Insecurity, and Hunger Under a Changing Climate: A Review. *J. Soil Sci. Plant Nutr.* **2024**, *24*, 74–101. [[CrossRef](#)]
60. Adimassu, Z.; Mul, M.; Owusu, A. Intra-seasonal rainfall variability and crop yield in the Upper East Region of Ghana. *Environ. Dev. Sustain.* **2023**, 1–20. [[CrossRef](#)]
61. Quaye-Ballard, J.A.; Okrah, T.M.; Andam-Akorful, S.A.; Awotwi, A.; Antwi, T.; Osei-Wusu, W.; Tang, X.; Quaye-Ballard, N.L. Spatiotemporal dynamics of rainfall in Upper East Region of Ghana, West Africa, 1981–2016. *SN Appl. Sci.* **2020**, *2*, 1675. [[CrossRef](#)]
62. Amede, T.; Awulachew, S.B.; Matti, B.; Yitayew, M. Managing Rainwater for Resilient Dryland Systems in Sub-Saharan Africa: Review of Evidences. In *Nile River Basin*; Springer: Cham, Switzerland, 2014; pp. 517–540.

- 
63. Nyssen, J.; Poesen, J.; Deckers, J. Land degradation and soil and water conservation in tropical highlands. *Soil Tillage Res.* **2009**, *103*, 197–202. [[CrossRef](#)]
  64. Vohland, K.; Barry, B. A review of in situ rainwater harvesting (RWH) practices modifying landscape functions in African drylands. *Agric. Ecosyst. Environ.* **2009**, *131*, 119–127. [[CrossRef](#)]

**Disclaimer/Publisher’s Note:** The statements, opinions and data contained in all publications are solely those of the individual author(s) and contributor(s) and not of MDPI and/or the editor(s). MDPI and/or the editor(s) disclaim responsibility for any injury to people or property resulting from any ideas, methods, instructions or products referred to in the content.